



Novel Green Synthesis of Zinc Oxide Nanoparticles Using Orange Waste and Its Thermal and Antibacterial Activity

A. A. Menazea^{1,2} · A. M. Ismail¹ · A. Samy³

Received: 1 April 2021 / Accepted: 16 July 2021 / Published online: 31 July 2021
© The Author(s), under exclusive licence to Springer Science+Business Media, LLC, part of Springer Nature 2021

Abstract

Zinc oxide nanoparticles (ZnO NPs) prepared via eco-friendly synthesis (using orange peels) are investigated. *Pseudomonas Aeruginosa* as a gram negative bacteria and *Bacillus subtilis* and *Staphylococcus Aureus* as a gram positive bacteria are used for studying antibacterial activity. XRD, FTIR-ATR and UV–Vis data confirmed the formation of ZnO NPs. Also, from XRD, UV–Vis data, optical band gap and HRTEM affirmed that the size of ZnO NPs prepared by chemical method is greater than that green synthesis methods. TGA and DTG indicates the high thermal stability of ZnO NPs prepared by chemical method than that prepared to green synthesis method. Antibacterial effect showed the slightly superior of the ZnO prepared by chemical method on the Prepared by green method at levels 50 and 100 ppm, while no differences found at 150 ppm in the *Pseudomonas aeruginosa* and *B. subtilis*. On the other hand, the comparable results for two zinc oxide nanoparticles in the *S. aureus*.

Keywords ZnO NPs · Orange peels · Chemical methods · Green method · Antibacterial activity

1 Introduction

Now days, scientists directed to use green methods that use environmentally sustainable materials that are compatible for pharmaceutical and medicine applications where the synthesis process does not use harmful chemicals. This method saves resources, non toxic and is cost-effective, which is advantages over other chemical processes. The biocompatibility of bio-inspired NPs in biomedicine and related fields provides very interesting applications [1]. Green synthesis of nanomaterial, created through the process of regulation, control, cleaning, and remediation. Such methods are used for minimize or prevent waste from accumulation, reduction of pollution as well as renewable of materials used in many application [2].

Nanomaterials are taken the attention of scientists in modern technology. These materials are classified as materials which their size less than about 100 nm. These materials are of interest because of they have unique optical, magnetic, electrical, antibacterial and many other properties that will have enormous uses on different fields of science [3–5]. Some nanomaterials exist naturally and some are created chemically; the latter are specifically developed for use in various application such as electronic products, clothing that is stain-resistant, medicines, feeds and foods [6, 7]. The chemical reactivity and strength of these nanomaterials are dependent on the surface area to volume ratios [8–10].

Nano-sized ZnO exhibits various morphologies and reveals strong antibacterial activity by a wider aspect of researchers over a wide range of bacterial species. In both microscale and nanoscale forms, ZnO is currently being studied as an antibacterial agent [11]. When particle size is decreased to the nanometer scale, ZnO exhibits substantial antimicrobial activity, then nano-sized ZnO will interact with the surface of bacterial surface and/or it is core where it reaches the cell and subsequently exhibits distinct bactericidal mechanisms. Most of the interactions between these distinctive materials and bacteria are toxic and have been used for antimicrobial applications, such as in the food industry [12]. One of the most productive fruits in the world

✉ A. A. Menazea
aanter7@gmail.com

¹ Spectroscopy Department, National Research Centre,
Giza 12622, Egypt

² Laser Technology Unit, National Research Centre,
Giza 12622, Egypt

³ Department of Animal Production, National Research Centre,
Giza 12622, Egypt

is the orange fruit. As the primary by-product of citrus, orange fruit peel is abundant in a number of anti-oxidants of natural origin. Orange peel is known to be used to prepare ZnONPs which are used as stabilizer [13, 14].

In present work, ZnO NPs will be prepared using chemical and green synthesis method. Structural, optical, morphology and antibacterial activity of the ZnO NPs that prepared by two different methods are studied.

2 Materials and Methods

2.1 Materials

Materials used: orange peel, from the wastes of the juice factories; Zinc nitrate [$\text{Zn}(\text{NO}_3)_2 \cdot 6\text{H}_2\text{O}$] as the zinc precursor (Sigma-Aldrich); sodium hydroxide (El-Gomhoria for chemicals), Poly ethylene glycol (300 M. wt), deionized water; nutrient agar medium (fluka, code:70148).

2.2 Preparation of Peel Extracts

Orange peel was washed then placed in oven at 60 °C for 12 h, after the complete dryness it was grounded to get fine powder. Afterwards, put 1:10 (W/V) powder to deionized water was stirred for 2 h at 40 °C water bath. Finally, the mixtures were centrifuged at 4 °C at 2000×g for 15 min. The resulting extract was stored in argon atmosphere for later use.

2.3 Synthesis of Zinc Oxide Nanoparticles

2.3.1 Green Sol–Gel Method

Mixing zinc nitrate (1 M) was a zinc precursor with orange peel extract as a reduced and surfactant reagent under vigorous stirrer for 2 h. After that, the white precipitate was obtained to separate it made centrifugation at 3000×g for 15 min. the precipitate was dried at 60 °C overnight.

2.3.2 Sol–Gel Chemical Method

Mixing zinc nitrate (1 M) was a zinc precursor with sodium hydroxide as a reduced reagent in a deionized water which is mixed before with polyethylene glycol (300 M. wt) as a surfactant reagent under vigorous stirrer for 2 h. After that, the white precipitate was obtained, to separate it made centrifugation at 3000×g for 15 min. the precipitate was dried at 60 °C overnight.

Two different samples of nano zinc oxide produced were calcinated at 350 °C, then the samples ready to be characterized.

2.4 Measurement Techniques

X-ray diffraction (XRD) is performed PANalytical X'Pert Pro target Cu-K α with secondary monochromator Holland radiation, the tube operating at 45 kV with 0.1540 nm wavelength over a 2 θ range of (5°–80°). FTIR-ATR spectral data are collected using Vertex 80 Bruker (made in Germany) at room temperature in the range 4000–400 cm⁻¹. UV/Vis. spectral data collected using Jasco V-630 spectrophotometer in the range 200–1000 nm at room temperature. High-Resolution Transmission Electron Microscope (HRTEM) was performed by JEM-2100F electron microscope with accelerating voltage of 200 kV. Thermogravimetric analysis (TGA) and its derivative (DTG) using A Perkin-Elmer TGA-7 from room temperature up to 1000 °C with heating rate of 10 °C/min.

2.5 Antimicrobial Assay of Zinc Oxide Nanoparticles

The antimicrobial potential of the Zinc oxide nanoparticles synthesized from the two different methods. The pathogenic microorganisms used in this study included three bacterial strains *Pseudomonas aeruginosa* (ATCC27853), *Bacillus subtilis* (ATCC 6633), *Staphylococcus aureus* (ATCC 6538). Qualitative evaluations were carried out in nutrient agar plates according to [15, 16]. The inoculation of all microorganisms was prepared from fresh overnight broth-cultures that were incubated at 37 °C [17]. The inoculum size of these pathogenic strains was prepared and adjusted to approximately 0.5 McFarland standard (1.5×10^8 CFU/mL), 25.0 μL of bacterial suspensions were inoculated into each plate containing 20.0 mL of the sterile nutrient agar medium (NA). After the media cooled and solidified, the prepared samples were applied on the surface of that inoculated agar plates which prepared previously at three levels 50, 100 and 150 ppm. These seeded plates were placed in the refrigerator for 1 h, followed by incubation at 37 °C for 24 h and zones of inhibition (ZI) were measured in mm [16].

3 Results and Discussions

3.1 X-Ray Diffraction (XRD)

XRD is a powerful technique for estimating the structure of organic, inorganic and metal oxide materials. Also, it helps for identifying the crystal size and crystallinity of materials. Figure 1 shows XRD of ZnO NPs by using chemical method and green synthesis method. As seen ZnO NPs using chemical method, there are diffraction peaks which has a crystalline structure at $2\theta = 31.6^\circ, 34.4^\circ,$

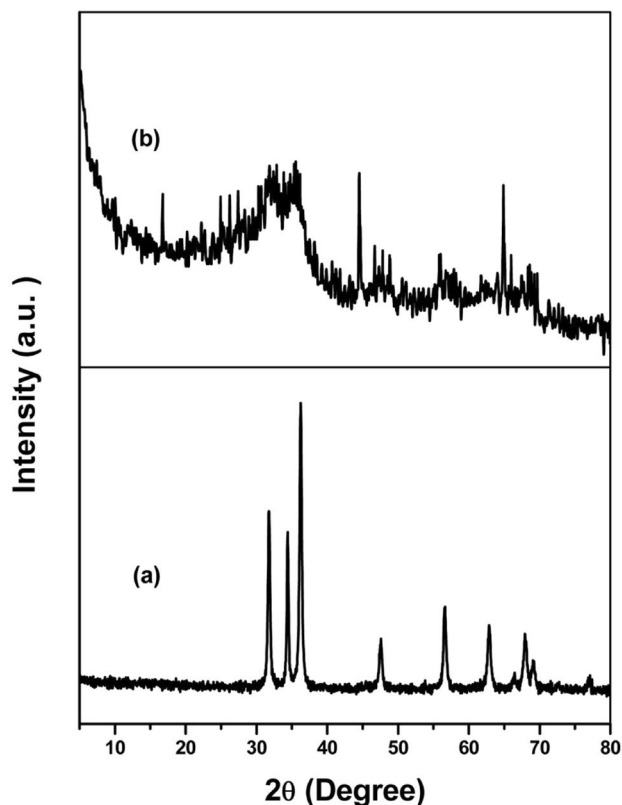


Fig. 1 XRD of ZnO NPs prepared by **a** chemical and **b** green synthesis methods

36.2°, 47.5°, 56.6°, 62.8° and 67.9° which corresponded to lattice planes (100), (002), (101), (102), (110), (103) and (112) [18–20] respectively which corresponds to reference code number 01-075-9742 that exhibited a hexagonal structure with no other any other phases was observed. While for ZnO prepared using green synthesis method, the diffraction peaks have less crystal structure compared the ZnO prepared by chemical method at $2\theta = 31.8^\circ$, 44.4° , 64.8° and 67.6° . The difference between the crystalline diffraction peaks of the two methods because of differences in crystal size and arrangement of atoms inside ZnO structure.

The average crystallite size was calculated using the Debye–Scherrer equation [21]

$$C = K\lambda/\beta\cos\theta \quad (1)$$

where C is the crystal size, k is a constant (0.915), λ is the X-ray wavelength and equal to 0.154 nm, β is the full width at half maximum (FWHM) of the diffraction peak (in radian) and θ is the Bragg's diffraction angle (in degree) of the peak maximum. The average crystal size of ZnO NPs was found to be 26 nm and 2.8 nm for chemical and green synthesis method respectively.

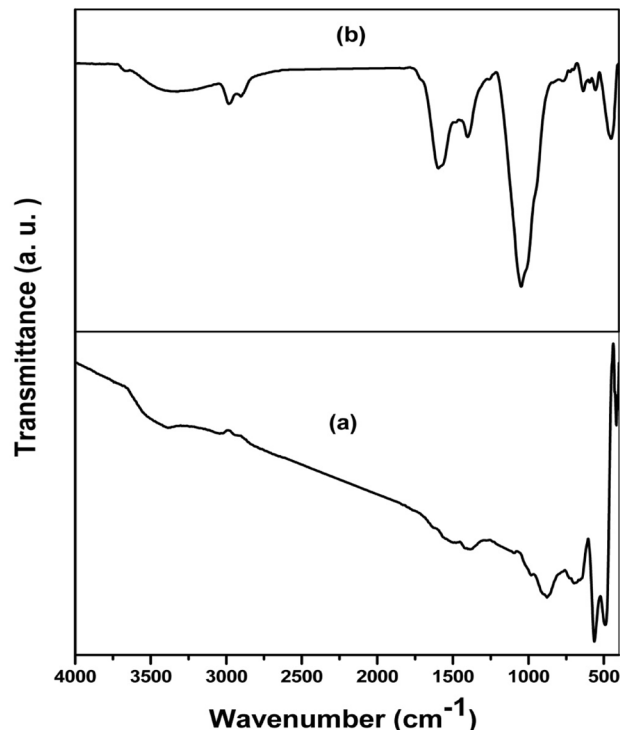


Fig. 2 FTIR-ATR of ZnO NPs prepared by **a** chemical and **b** green synthesis methods

The density of dislocation is defined as the length of dislocation lines per unit volume of the crystal. In materials science, a dislocation inside a crystal structure is a crystallographic defect, or irregularity. Many of the properties of materials are greatly influenced by the presence of dislocations. Other dislocations present in the sample hinder the movement of a dislocation. Therefore, a greater density of dislocation means a larger hardness. To evaluate the dislocation density, an analysis of the X-ray line profile was used. The dislocation density (δ) was calculated in the sample [22].

$$\delta = 1/C^2 \quad (2)$$

The dislocation density for ZnO NPs synthesized from chemical and green methods are found to be $1.47 \times 10^{-3} \text{ nm}^{-2}$ and $127.5 \times 10^{-3} \text{ nm}^{-2}$.

3.2 Fourier Transform Infrared-Attenuated Total Reflection (FTIR-ATR)

Figure 2 shows that FTIR-ATR of ZnO NPs prepared by chemical and green methods. Figure 2a shows bands at 3404 cm^{-1} and at 1391 cm^{-1} which are related to O–H stretching and bending vibration from adsorbed water from air and atmospheric moisture [23]. The absorption at

877 cm^{-1} is due to the formation of tetrahedral coordination of Zn. The bands at 564 cm^{-1} , 491 cm^{-1} and 417 cm^{-1} are assigned to metal–oxygen bond which is Zn–O bond [24, 25]. While in Fig. 2b, for ZnO NPs prepared by green synthesis method, the stretching vibration of O–H group is seen at 3367 cm^{-1} . C–H stretching vibration is seen at 2984 cm^{-1} . The band at 1596 cm^{-1} and 1401 cm^{-1} is corresponded to the stretching vibration of carbonyl and carboxylate group. The C–O stretching vibration is seen at 1047 cm^{-1} . The bands at 637 cm^{-1} , 557 cm^{-1} and 454 cm^{-1} confirmed the presence of ZnO NPs which are attributed to Zn–O [26–28]. The difference in position of wavenumber and appearance of other peaks are related to difference in method of preparation, arrangement of molecules and particle.

3.3 Optical Properties

UV–Vis of ZnO NPs prepared by chemical and green synthesis method is illustrated in Fig. 3. As seen in Fig. 3 that ZnO NPs prepared by chemical method, there is a sharp peak at 375 nm and its agreed with that reported in previous literature [29–32] and for ZnO NPs prepared by green synthesis method, there is fine peak at 348 nm [33] which confirmed the formation of ZnO NPs. As observed the maximum absorption wavelength for ZnO NPs prepared by chemical method is larger than that for ZnO NPs prepared by green synthesis method that mean that the size

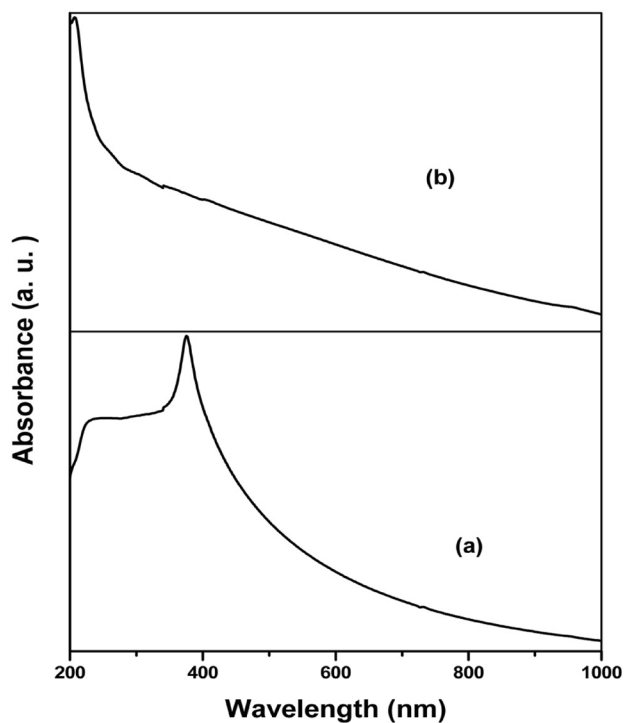


Fig. 3 UV–Vis spectra of ZnO NPs prepared by **a** chemical and **b** green synthesis methods

of nanoparticles is large for chemical method compared with that prepared by green method and that agreed with XRD results.

The absorption coefficient (α) for ZnO NPs prepared by chemical and green synthesis method is calculated using the following equation [34]

$$\alpha(\lambda) = \frac{2.303}{D} A \quad (3)$$

where D and A are the thickness and absorbance of sample. Figure 4 shows the plot between α and $h\nu$ for ZnO NPs prepared by chemical and green synthesis method, values of absorption edge are determined by extrapolating the linear portion of the plot with photon energy ($h\nu$). Values of absorption edge obtained are 1.55 eV and 3.86 eV for ZnO NPs prepared by chemical and green synthesis method, respectively. Direct band gap energy is calculated using tauch relationship as follow [35]:

$$(\alpha h\nu)^2 = \rho (h\nu - E_g) \quad (4)$$

where ρ and E_g are constant and band gap energy. Figure 5 shows the plot between $(\alpha h\nu)^2$ and $h\nu$, values of E_g are obtained by extrapolating the linear portion of the plot with photon energy ($h\nu$). As seen values of band gap for ZnO NPs prepared by chemical and green synthesis method are 2.71 eV and 4.49 eV, respectively. This mean that the particle size increases with decreasing the band gap energy [32], also the degree of disordering for ZnO NPs prepared by chemical method is higher than that prepared by green synthesis method.

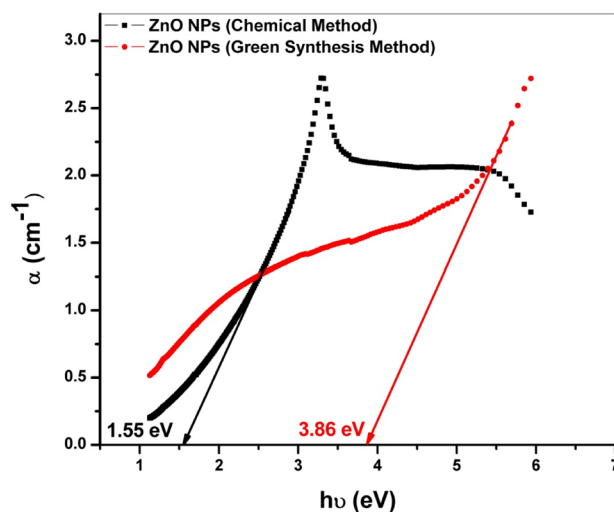


Fig. 4 Relation between α and $h\nu$ for ZnO NPs prepared by chemical and greensynthesis methods

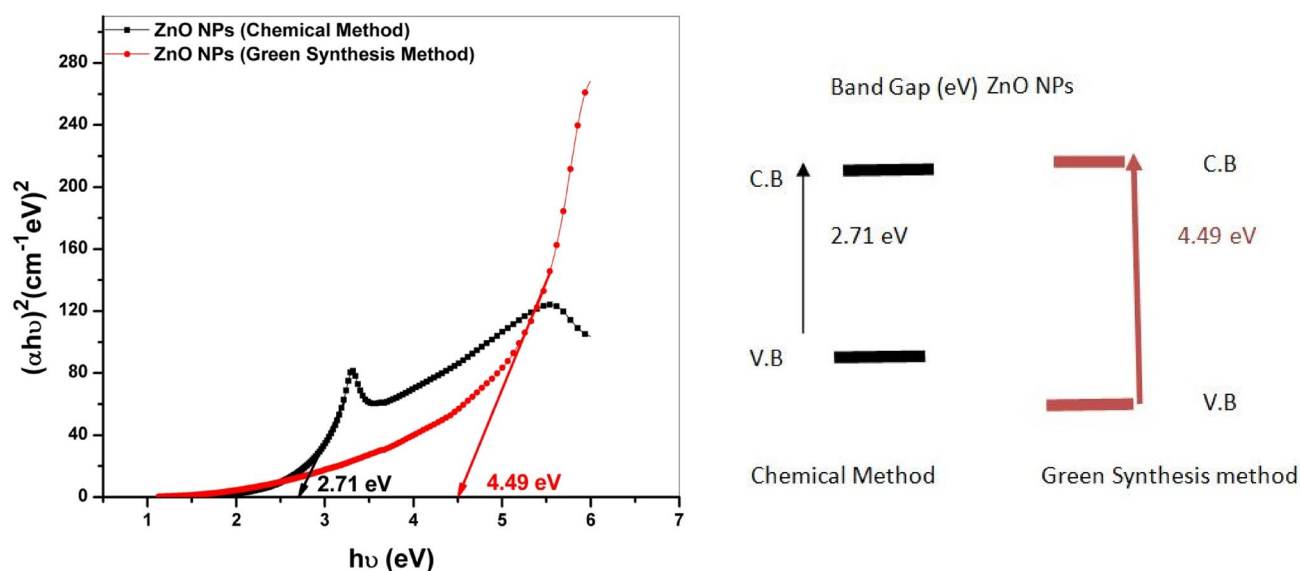


Fig. 5 Relation between $(\alpha h\nu)^2$ and $h\nu$ for ZnO NPs prepared by chemical and green synthesis methods

3.4 High Resolution Transmission Electron Microscope (HRTEM)

Figure 6 shows HRTEM of ZnO NPs prepared by chemical and green synthesis method. As seen in Fig. 6a that ZnO NPs prepared by chemical method have large clusters with irregular shapes like pseudospherical shape and some of them has straight borders that smoothed with cubic shape with average size ranges from 20 to 60 nm while ZnO prepared by green synthesis method have small size with spherical shape that have been coagulated in large blocks ranged from 2–6 nm. The difference in the diameters observed for the study of XRD and HRTEM may be due to the likely inherent restriction associated with the use of XRD, since it reflects only the average diameter of the particle size that caused diffraction (crystal size) while HRTEM measure the particle size that taken in certain area.

3.5 Thermogravimetric Analysis (TGA) and It's Derivative (DTG)

TGA and DTG of ZnO NPs prepared by chemical method and green synthesis method are seen in Fig. 7. The first decomposition losses for the two samples from 22 to 240 °C are regarded to dehydration of water adsorbed on the surface. The second decomposition losses from 240 to 550 °C are attributed to decomposition of $\text{Zn}(\text{OH})_2$ to ZnO NPs. The third decomposition losses from 550 to 1000 °C are regarded to the decomposition of the residual surfactant. As seen that the total weight loss for ZnO NPs prepared by chemical method and green synthesis method are 26% and 52%, respectively that is mean that

the thermal stability of ZnO NPs prepared by chemical method is more stable than that prepared to green synthesis method regarding to the high purity of ZnO NPs prepared by chemical method and these results agreed with XRD data.

3.6 Antimicrobial Activity

Antimicrobial activity for zinc oxide nanoparticles synthesized by two different methods; chemical method (a) and Green method (b) at three levels 50, 100, 150 ppm are shown in Fig. 8. The results showed that the inhibition zone of *B. subtilis* for ZnONPs at 50, 100 and 150 ppm Produced by green method gives 10, 13 and 20 mm while the ZnO NPs produced by chemical method give 18, 20 and 21 mm, respectively. In addition, the inhibition zone of *Pseudomonas aeruginosa* for ZnO NPs at 50, 100 and 150 ppm produced by green method gives 11, 15 and 20 mm while the ZnO NPs produced by chemical method give 18, 21 and 22 mm, respectively. On the other hand the comparable results found for the inhibition zone of *S. aureus* for ZnO NPs at 50, 100 and 150 ppm Produced by green method gives 10, 10 and 13 mm while the ZnO NPs produced by chemical method give 11, 10 and 13 mm, respectively. The results showed the slightly superior of the ZnO prepared by chemical method on the Prepared by green method at levels 50 and 100 ppm, while no differences found at 150 ppm in the *Pseudomonas aeruginosa* and *B. subtilis*. On the other hand, the comparable results for two zinc oxide nanoparticles in the *S. aureus* (Fig. 9) [29, 36, 37].

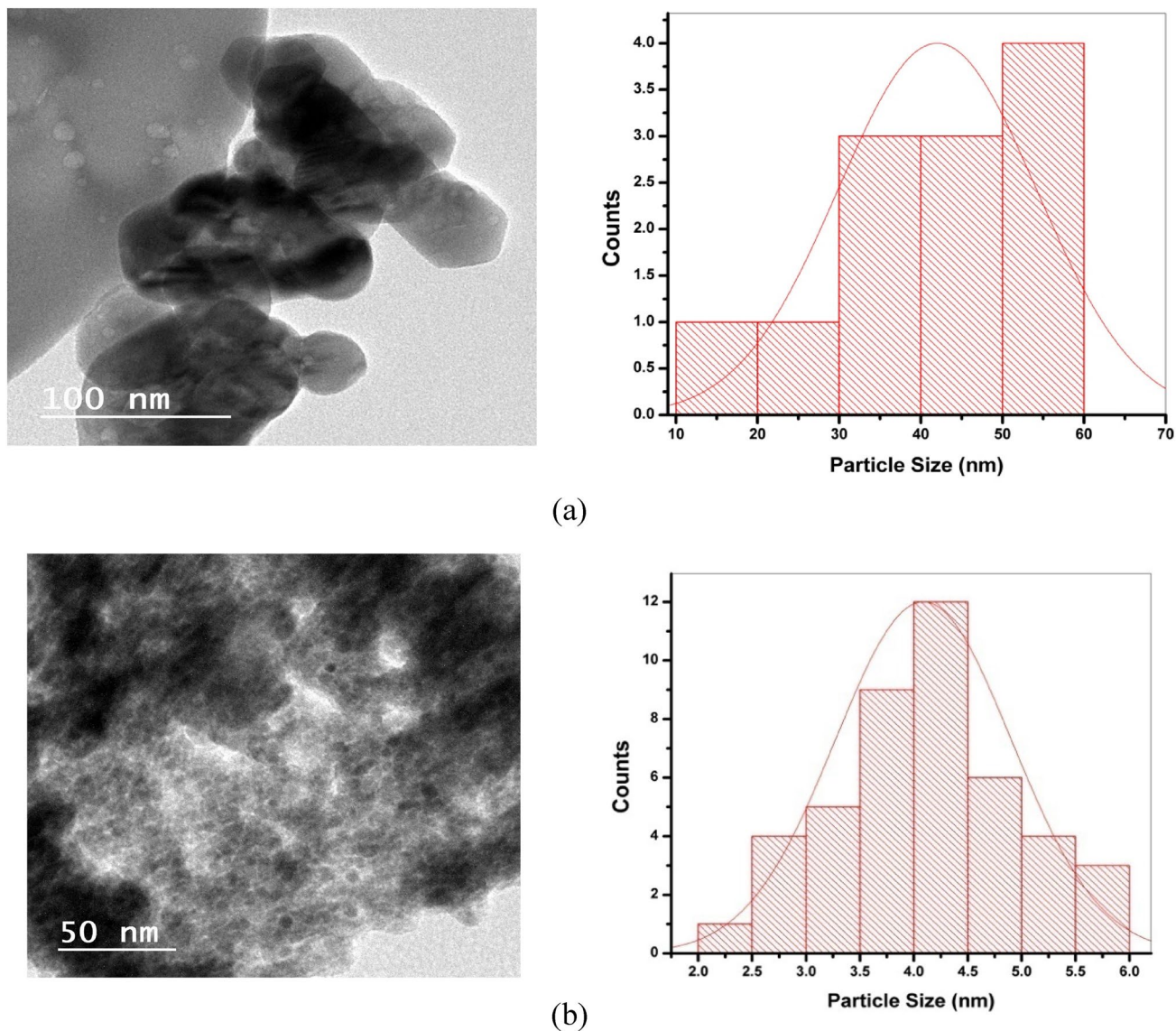


Fig. 6 HRTEM of ZnO NPs prepared by **a** chemical and **b** green synthesis methods

4 Conclusion

Structural, optical, morphological and antibacterial activity of ZnO NPs prepared by chemical method and green synthesis methods (using orange peels) are studied. XRD confirmed the formation of ZnO NPs with crystal size 26 nm and 2.8 nm for chemical method and green synthesis methods respectively. Bands appeared in range $600\text{--}400\text{ cm}^{-1}$ in FTIR-ATR proved the presence of metal oxide nanoparticles (ZnO NPs). UV-Vis data confirmed

the formation of ZnO NPs at 375 nm and 348 nm for chemical method and green synthesis methods respectively. Band gap energy and HRTEM for ZnO NPs prepared by chemical method are higher than that prepared by green synthesis method and that agreed with XRD results. The thermal stability of ZnO NPs prepared by chemical method is more stable than that prepared to green synthesis method. The comparable antibacterial effect was detected between two different ZnO NPs at 150 ppm on the *Pseudomonas aeruginosa*, *B. subtilis* and *S. aureus*.

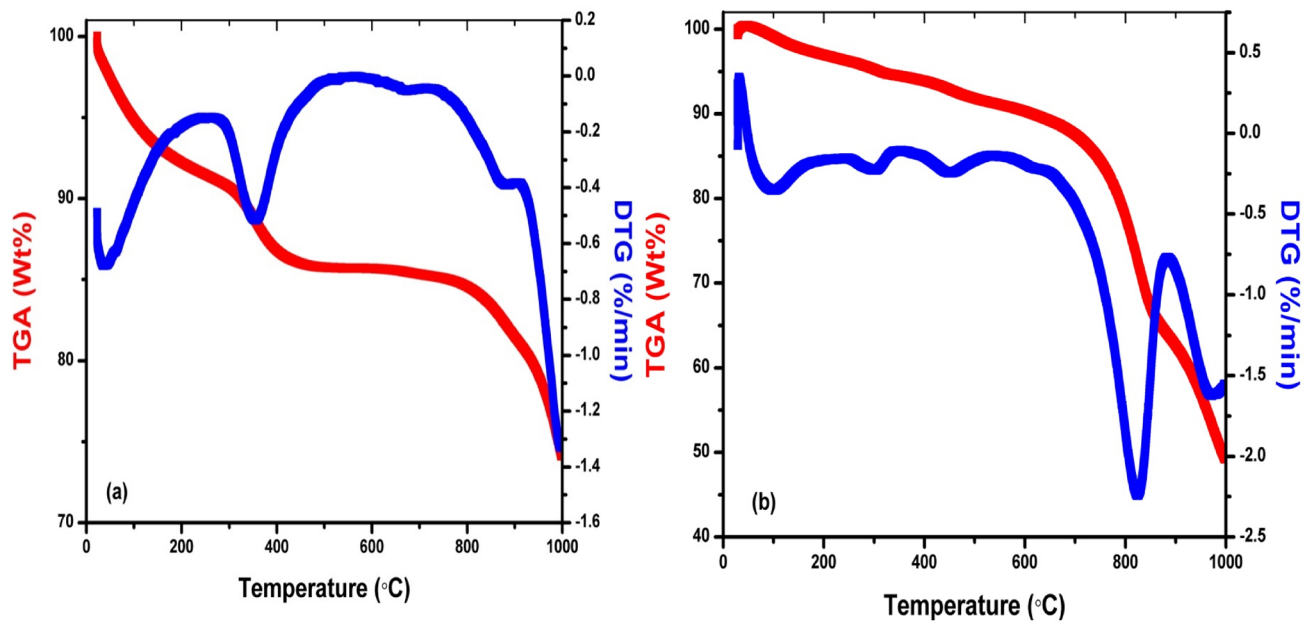


Fig. 7 TGA and DTG for ZnO NPs prepared by **a** chemical and **b** green synthesis methods

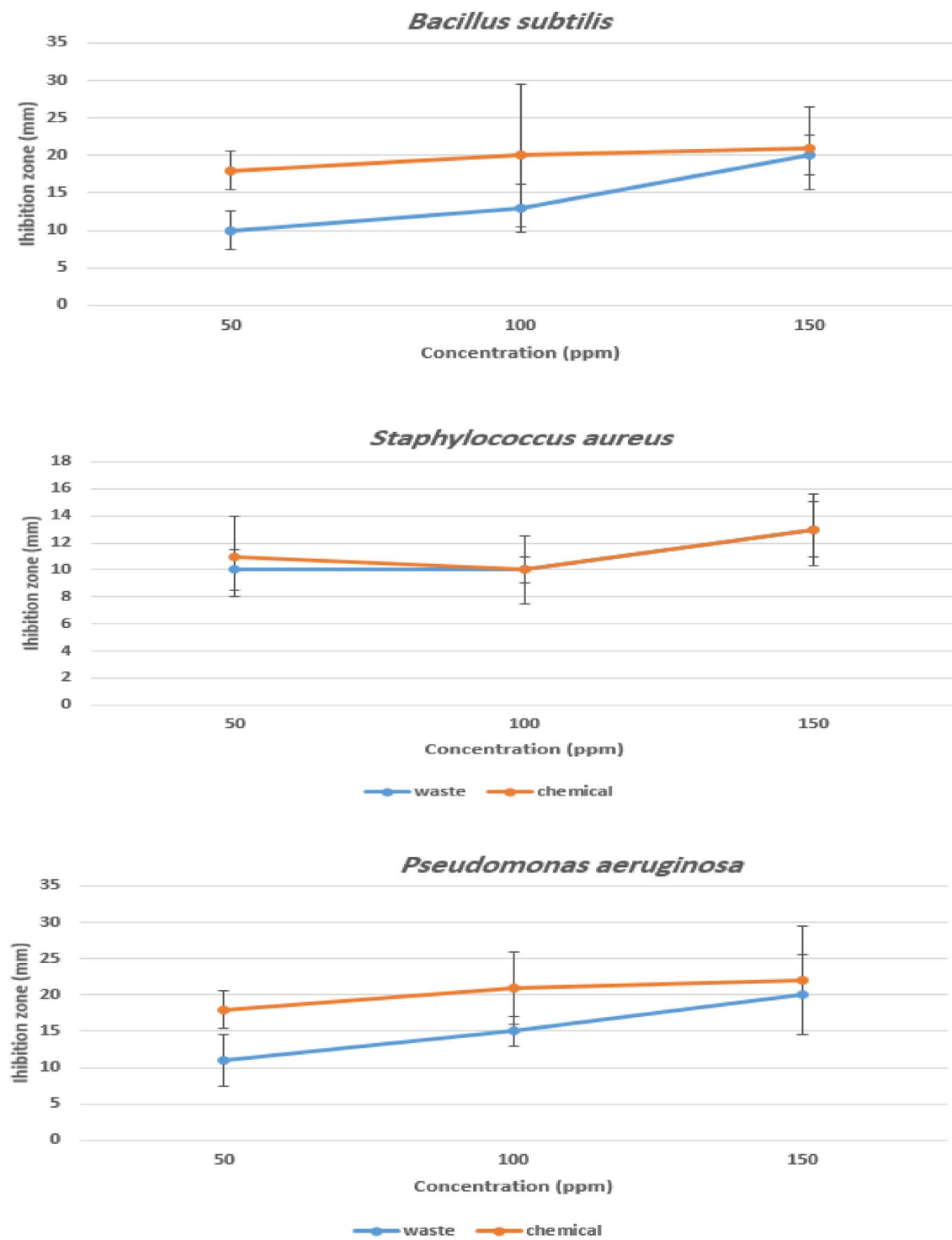


Fig. 8 Antimicrobial activity for ZnO NPs prepared by **a** chemical and **b** green synthesis methods

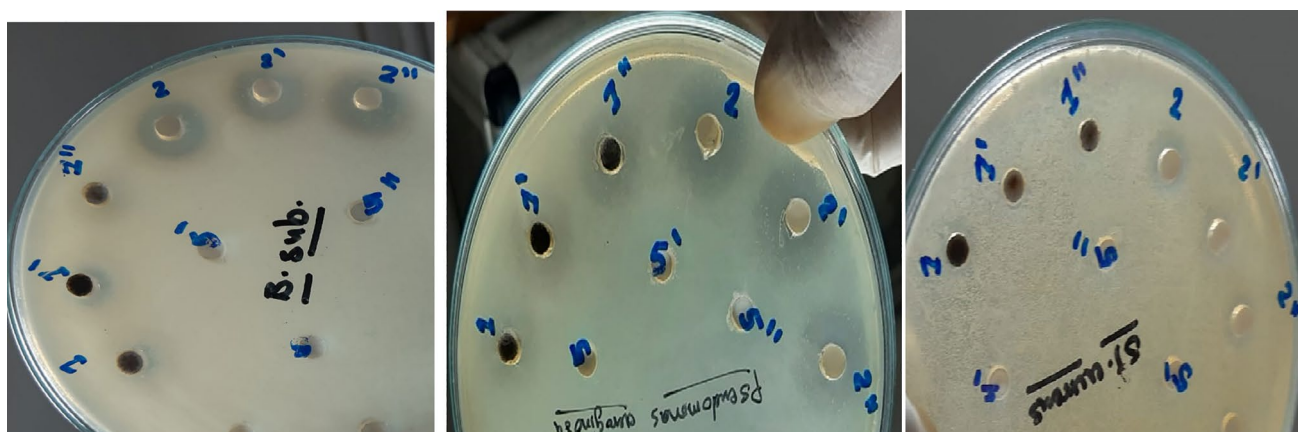


Fig. 9 Antimicrobial activity for ZnO NPs prepared by (1) green and (2) chemical synthesis methods

Acknowledgements This study was financially supported by National Research Centre of Egypt through internal research Project No. 12020216.

Declarations

Conflict of interest The authors declare that they have no conflict of interest.

References

1. J. Huang, L. Lin, D. Sun, H. Chen, D. Yang, Q. Li, Bio-inspired synthesis of metal nanomaterials and applications. *Chem. Soc. Rev.* **44**(17), 6330–6374 (2015). <https://doi.org/10.1039/c5cs00133a>
2. J. Singh, T. Dutta, K. Kim, M. Rawat, P. Samddar, P. Kumar, ‘Green’ synthesis of metals and their oxide nanoparticles: applications for environmental remediation. *J. Nanobiotechnol.* (2018). <https://doi.org/10.1186/s12951-018-0408-4>
3. U.T. Khatoon, G.N. Rao, M.K. Mohan, A. Ramanaviciene, A. Ramanavicius, Comparative study of antifungal activity of silver and gold nanoparticles synthesized by facile chemical approach. *J. Environ. Chem. Eng.* **6**(5), 5837–5844 (2018)
4. N. Anzar, R. Hasan, M. Tyagi, N. Yadav, J. Narang, Carbon nanotube-A review on synthesis, properties and plethora of applications in the field of biomedical science. *Sens. Int.* **1**, 100003 (2020)
5. U.T. Khatoon, G.N. Rao, K.M. Mohan, A. Ramanaviciene, A. Ramanavicius, Antibacterial and antifungal activity of silver nanospheres synthesized by tri-sodium citrate assisted chemical approach. *Vacuum* **146**, 259–265 (2017)
6. M.A. Mohamed, H.M.A. Hassan, A. Samy, M.O. Abd-Elsamee, A.E. El-Sherbiny, Carcass characteristics and bone measurements of broilers fed nanocalcium phosphate containing diets. *Asian J. Anim. Vet. Adv.* **11**(8), 484–490 (2016)
7. H.M.A. Hassan, A. Samy, A.E. El-Sherbiny, M.A. Mohamed, M.O. Abd-Elsamee, Application of nano-dicalcium phosphate in broiler nutrition: performance and excreted calcium and phosphorus. *Asian J. Anim. Vet. Adv.* **11**, 477–483 (2016)
8. P. Navya, H. Daima, Rational engineering of physicochemical properties of nanomaterials for biomedical applications with nanotoxicological perspectives. *Nano Converg.* (2016). <https://doi.org/10.1186/s40580-016-0064-z>
9. S. Mourdikoudis, R. Pallares, N. Thanh, Characterization techniques for nanoparticles: comparison and complementarity upon studying nanoparticle properties. *Nanoscale* **10**(27), 12871–12934 (2018). <https://doi.org/10.1039/c8nr02278j>
10. C. Wang, L. Zhang, W. Su, Z. Ying, J. He, L. Zhang et al., Zinc oxide nanoparticles as a substitute for zinc oxide or colistin sulfate: effects on growth, serum enzymes, zinc deposition, intestinal morphology and epithelial barrier in weaned piglets. *PLoS ONE* **12**(7), e0181136 (2017). <https://doi.org/10.1371/journal.pone.0181136>
11. A. Sirelkhatim, S. Mahmud, A. Seeni, N. Kaus, L. Ann, S. Bakhor et al., Review on zinc oxide nanoparticles: antibacterial activity and toxicity mechanism. *Nano-Micro Lett.* **7**(3), 219–242 (2015). <https://doi.org/10.1007/s40820-015-0040-x>
12. J.D. de Amorim, K.C. de Souza, C.R. Duarte, D.I. da Silva, F.D. Ribeiro, G.S. Silva, P.M. de Farias, A. Stingl, A.F. Costa, G.M. Vinhas, L.A. Sarubbo, Plant and bacterial nanocellulose: production, properties and applications in medicine, food, cosmetics, electronics and engineering. A review. *Environ. Chem. Lett.* **18**(3), 851–869 (2020)
13. O. Nava, C. Soto-Robles, C. Gómez-Gutiérrez, A. Vilchis-Nestor, A. Castro-Beltrán, A. Olivas, P. Luque, Fruit peel extract mediated green synthesis of zinc oxide nanoparticles. *J. Mol. Struct.* **1147**, 1–6 (2017). <https://doi.org/10.1016/j.molstruc.2017.06.078>
14. S. Alamdari, M. SasaniGhamsari, C. Lee, W. Han, H. Park, M. Tafreshi et al., Preparation and characterization of zinc oxide nanoparticles using leaf extract of *Sambucus*. *Appl. Sci.* **10**(10), 3620 (2020). <https://doi.org/10.3390/app10103620>
15. B.H. Joshi, R.M. Dhingani, Assessment and selection of multi-trait plant growth promoting bacteria associated with rice rhizosphere. *J. Pharmacogn. Phytochem.* **9**(2), 942–948 (2020)
16. F.A. Mostafa, A.A. Abd El Aty, E.R. Hamed, B.M. Eid, N.A. Ibrahim, Enzymatic, kinetic and anti-microbial studies on *Aspergillus terreus* culture filtrate and *Allium cepa* seeds extract and their potent applications. *Biocatal. Agric. Biotechnol.* **5**, 116–122 (2016)
17. W.S. El-serwy et al., Synthesis of new benzofuran derivatives and evaluation of their antimicrobial activities. *Res. J. Pharm. Biol. Chem. Sci.* **6**, 213–224 (2015)
18. D. Veer, R. Singh, H. Kumar, Structural and optical characterization of ZnO-TiO₂-SiO₂ nanocomposites synthesized by sol-gel

- technique. *Asian J. Chem.* **29**(11), 2391–2395 (2017). <https://doi.org/10.14233/ajchem.2017.20690>
19. W. Muhammad, N. Ullah, M. Haroon, B. Abbasi, Optical, morphological and biological analysis of zinc oxide nanoparticles (ZnO NPs) using *Papaversomniferum* L. *RSC Adv.* **9**(51), 29541–29548 (2019). <https://doi.org/10.1039/c9ra04424h>
 20. T.U.D. Thi, T.T. Nguyen, Y.D. Thi, K.H.T. Thi, B.T. Phan, K.N. Pham, Green synthesis of ZnO nanoparticles using orange fruit peel extract for antibacterial activities. *RSC Adv.* **10**(40), 23899–23907 (2020)
 21. S.K. Sen, U.C. Barman, M.S. Manir, P. Mondal, S. Dutta, M. Paul, M.A. Chowdhury, M.A. Hakim, X-ray peak profile analysis of pure and Dy-doped α -MoO₃ nanobelts using Debye-Scherrer, Williamson-Hall and Halder-Wagner methods. *Adv. Nat. Sci.: Nanosci. Nanotechnol.* **11**(2), 025004 (2020)
 22. E. Okpara, O. Fayemi, E. Sherif, H. Junaedi, E. Ebenso, Green wastes mediated zinc oxide nanoparticles: synthesis, characterization and electrochemical studies. *Materials* **13**(19), 4241 (2020). <https://doi.org/10.3390/ma13194241>
 23. G. Nagaraju, S. Udayabhanu, S. Prashanth, M. Shastri, K. Yathish et al., Electrochemical heavy metal detection, photocatalytic, photoluminescence, biodiesel production and antibacterial activities of Ag–ZnO nanomaterial. *Mater. Res. Bull.* **94**, 54–63 (2017). <https://doi.org/10.1016/j.materresbull.2017.05.043>
 24. N. Jayarambabu, S. Kumari, K. Venkateswara Rao, Y.T. Prabhu, Beneficial role of zinc oxide nanoparticles on green crop production. *Int. Res. Trends* **11**, 273–282 (2015)
 25. N.J. Usharani, R. Shringi, H. Sanghavi, S. Subramanian, S.S. Bhattacharya, Role of size, alio-/multi-valency and non-stoichiometry in the synthesis of phase-pure high entropy oxide (Co, Cu, Mg, Na, Ni, Zn) O. *Dalton Trans.* **49**(21), 7123–7132 (2020)
 26. P. Luque, C. Soto-Robles, O. Nava, C. Gomez-Gutierrez, A. Castro-Beltran, H. Garrafa-Galvez et al., Green synthesis of zinc oxide nanoparticles using *Citrus sinensis* extract. *J. Mater. Sci.: Mater. Electron.* **29**(12), 9764–9770 (2018). <https://doi.org/10.1007/s10854-018-9015-2>
 27. M. Rezaei, A. Nezamzadeh-Ejhiha, The ZnO–NiO nano-composite: a brief characterization, kinetic and thermodynamic study and study the Arrhenius model on the sulfasalazine photodegradation. *Int. J. Hydrog. Energy* **45**(46), 24749–24764 (2020)
 28. A. Samy, A.E. El-Sherbiny, A.A. Menazea, Green synthesis of high impact zinc oxide nanoparticles. (The first international conference on molecular modeling and spectroscopy 19–22 February, 2019). *Egypt. J. Chem.* **62**, 29–37 (2019)
 29. A. Ismail, A. Menazea, H. Kabary, A. El-Sherbiny, A. Samy, The influence of calcination temperature on structural and antimicrobial characteristics of zinc oxide nanoparticles synthesized by Sol-Gel method. *J. Mol. Struct.* **1196**, 332–337 (2019). <https://doi.org/10.1016/j.molstruc.2019.06.084>
 30. A.M. Mostafa, A.A. Menazea, Laser-assisted for preparation ZnO/CdO thin film prepared by pulsed laser deposition for catalytic degradation. *Radiat Phys Chem* **176**, 109020 (2020)
 31. A. Singh, M. Kaushik, Physicochemical investigations of zinc oxide nanoparticles synthesized from *Azadirachta Indica* (Neem) leaf extract and their interaction with Calf-Thymus DNA. *Results Phys.* **13**, 102168 (2019)
 32. A.A. Menazea, N.S. Awwad, Antibacterial activity of TiO₂ doped ZnO composite synthesized via laser ablation route for antimicrobial application. *J. Mater. Res. Technol.* **9**(4), 9434–9441 (2020)
 33. D. Biron, V. Santos, C. Bergmann, Synthesis and characterization of zinc oxide obtained by combining zinc nitrate with sodium hydroxide in polyol medium. *Mater. Res.* (2020). <https://doi.org/10.1590/1980-5373-mr-2020-0080>
 34. T. Siddaiah, P. Ojha, N. Kumar, C. Ramu, Structural, optical and thermal characterizations of PVA/MAA: EA polyblend films. *Mater. Res.* (2018). <https://doi.org/10.1590/1980-5373-mr-2017-0987>
 35. J. Tauc (ed.), *Amorphous and Liquid Semiconductor* (Plenum Press, New York, 1974)
 36. A. Raja, S. Ashokkumar, R.P. Marthandam, J. Jayachandiran, C.P. Khatiwada, K. Kaviyarasu, R.G. Raman, M. Swaminathan, Eco-friendly preparation of zinc oxide nanoparticles using *Tabernaemontana divaricata* and its photocatalytic and antimicrobial activity. *J. Photochem. Photobiol. B* **181**, 53–58 (2018)
 37. N. Bala, S. Saha, M. Chakraborty, M. Maiti, S. Das, R. Basu, P. Nandy, Green synthesis of zinc oxide nanoparticles using *Hibiscus subdariffa* leaf extract: effect of temperature on synthesis, anti-bacterial activity and anti-diabetic activity. *RSC Adv.* **5**(7), 4993–5003 (2015)

Publisher's Note Springer Nature remains neutral with regard to jurisdictional claims in published maps and institutional affiliations.